X-ray Diffraction of a Cysteine-Containing Bacteriorhodopsin Mutant and Its Mercury Derivative. Localization of an Amino Acid Residue in the Loop of an Integral Membrane Protein†

Mark P. Krebs,‡ Wolfgang Behrens,§ Ramin Mollaaghababa,‡ H. Gobind Khorana,*,‡ and Maarten P. Heyn§

Departments of Biology and Chemistry, Massachusetts Institute of Technology, 77 Massachusetts Avenue, Cambridge, Massachusetts 02139, and Biophysics Group, Department of Physics, Freie Universität Berlin, Arnimallee 14, D-14195 Berlin 33, Germany

Received August 27, 1993®

ABSTRACT: We have used heavy-atom labeling and X-ray diffraction to localize a single amino acid in the integral membrane protein bacteriorhodopsin (bR). To provide a labeling site, we used the bR mutant, A103C, which contains a unique cysteine residue in the short loop between transmembrane α-helices C and D. The mutant protein was expressed in and purified from *Halobacterium halobium*, where it forms a two-dimensional crystalline lattice. In the lattice form, the protein reacted with the sulfhydryl-specific reagent *p*-chloromercuribenzoate (*p*-CMB) in a 1:0.9 stoichiometry to yield the *p*-mercuribenzoate derivative (A103C-MB). The functional properties of A103C and A103C-MB, including the visible absorption spectrum, light-dark adaptation, photocycle, and proton release kinetics, were similar to those of wild-type bR. X-ray diffraction experiments demonstrated that A103C and A103C-MB membranes have the same hexagonal protein lattice as wild-type purple membrane. Thus, neither the cysteine substitution nor mercury labeling detectably affected bR structure or function. By using Fourier difference methods, the in-plane position of the mercuribenzoate label was calculated from intensity differences in the X-ray diffraction patterns of A103C and A103C-MB. This analysis revealed a well-defined mercury peak located between α-helices C and D. The approach reported here offers promise for refining the bR structural model, for monitoring conformational changes in bR photointermediates, and for studying the structure of other proteins in two-dimensional crystals.

Structural studies of integral membrane proteins have progressed more slowly than studies of soluble proteins, largely because of the difficulty in obtaining well-ordered three-dimensional crystals. To circumvent this problem, electron crystallography techniques (Amos et al., 1982; Henderson et al., 1986, 1990) have been developed to analyze two-dimensional crystals of integral membrane proteins in a lipid bilayer (Kühlbrandt, 1992). By using these techniques, structures of 6-Å resolution or more have been obtained for a number of proteins (Kühlbrandt, 1992). Recent examples include the nicotinic acetylcholine receptor (Unwin, 1993), the calcium ATPase of the sarcoplasmic reticulum (Toyoshima et al., 1993), and bovine rhodopsin (Schertler et al., 1993).

The most successful application of this approach has been the electron diffraction studies of bacteriorhodopsin (bR)[1] from *Halobacterium halobium* (Henderson et al., 1990). This retinal-containing integral membrane protein functions as a light-driven pump in which isomerization of the chromophore is coupled to proton translocation (Stoeckenius et al., 1979; Stoeckenius & Bogomolni, 1982; Mathies et al., 1992). Electron diffraction studies of bR have been facilitated because the protein can be isolated from *H. halobium* in the purple membrane, a two-dimensional crystalline lattice of hexagonal symmetry containing three bR molecules per unit cell. In the structural model derived from studies of the purple membrane, bR consists of a bundle of seven transmembrane α-helices that forms a binding pocket for the retinal chromophore (Henderson et al., 1990). The model has a resolution of 3.5 Å in the plane of the membrane and 7–10 Å in the vertical dimension.

The low-to-moderate resolution of electron crystallography studies results in considerable uncertainty in the derived structural models. Consequently, structural information obtained from other techniques is required for modeling. In the case of bR, biochemical, spectroscopic, nuclear magnetic resonance, neutron diffraction, and mutagenesis data were used to position the retinal chromophore and to orient several of the transmembrane α-helices (Henderson et al., 1990). However, such information is generally not available for the entire protein, so some regions cannot be modeled reliably. In bR, these include the amino and carboxy termini and the loops connecting the transmembrane α-helices. Further studies are required to refine the structure of these regions.

We demonstrate here an approach for localizing single amino acids in two-dimensional crystals of an integral membrane protein. Site-directed mutagenesis is used to produce a mutant protein containing a unique cysteine residue. The sulfhydryl group forms a specific, high-affinity complex with mercury-containing compounds that can be localized by X-ray diffraction. An X-ray powder diffraction pattern of a two-dimensional crystal can be combined with phases derived from electron imaging to yield a low-resolution projection map (Plöhn & Büldt, 1986). By using Fourier difference

† This work was supported by Grant GM28289 from the National Institutes of Health (H.G.K.) and by Grant 03-HE3FUB from the Bundesministerium für Forschung und Technologie (M.P.H.).

* Author to whom correspondence should be addressed.

‡ Massachusetts Institute of Technology.

§ Freie Universität Berlin.

® Abstract published in *Advance ACS Abstracts,* November 1, 1993.

[1] Abbreviations: bR, bacteriorhodopsin; *p*-CMB, *p*-chloromercuribenzoate; A103C, bR mutant containing an alanine to cysteine substitution at position 103; A103C-MB, mercuribenzoate derivative of the A103C mutant.

0006-2960/93/0432-12830$04.00/0

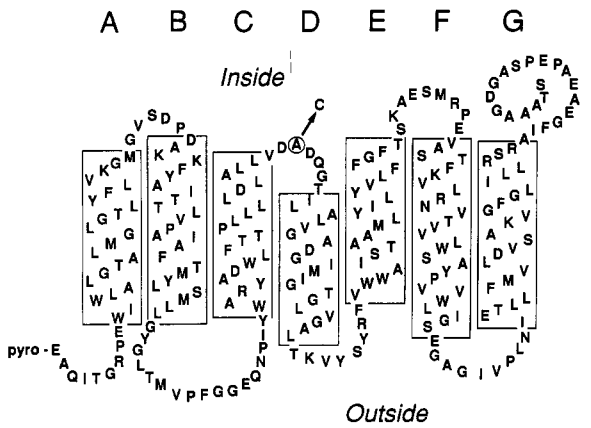

FIGURE 1: Secondary structure map of bacteriorhodopsin based on the model of Henderson et al. (1990). Boxed regions labeled A–G correspond to the transmembrane α-helices. The circled residue indicates Ala-103, which was substituted with cysteine in this study.

methods, the location of the labeling site is obtained from the difference in the diffraction amplitudes in the presence and absence of the heavy atom. The use of site-specific mutagenesis to introduce heavy-atom labeling sites has been effective for structural studies of proteins that form three-dimensional crystals (Dao-Pin et al., 1987; Tucker et al., 1989; Stock et al., 1989; Klein et al., 1990).

We used this strategy to localize an amino acid residue within a loop region of bR. The bR mutant A103C (Greenhalgh et al., 1991) contains a unique cysteine residue in the C–D loop (Figure 1). We used a gene replacement procedure developed for *H. halobium* (Krebs et al., 1993) to express and isolate the A103C protein in a two-dimensional crystalline lattice. In this form, the purified protein was labeled efficiently with the sulfhydryl-specific reagent *p*-chloromercuribenzoate (*p*-CMB). X-ray diffraction revealed a single mercury label at the expected site between transmembrane α-helices C and D (Henderson, 1990; Engelman et al., 1980). We discuss the potential application of this approach for refining the bR structural model, for studying conformational changes during the bR photocycle, and for determining the structure of other integral membrane proteins.

MATERIALS AND METHODS

Expression and Purification of A103C. A plasmid carrying the A103C mutation in the bacterioopsin gene was constructed as described (Krebs et al., 1993) by replacing the Asp718–BspHI fragment from the native gene in pMPK62 (Krebs et al., 1993) with the corresponding synthetic fragment from pSB02 (Nassal et al., 1987) containing the A103C mutation (Greenhalgh et al., 1991). A recombinant *H. halobium* strain producing A103C was constructed with this plasmid as described (Krebs et al., 1993). A103C was expressed in this strain and purified in a membrane form as reported previously (Krebs et al., 1991). The purity of A103C in membranes was determined by densitometric scanning of a Coomassie-stained, sodium dodecyl sulfate/14% polyacrylamide gel. Wild-type bR was similarly prepared from MPK1 (Krebs et al., 1991) or from an *H. halobium* strain that contains a synthetic Asp718–BspH1 fragment in the bacterioopsin gene (Krebs et al., 1993).

Heavy-Atom Labeling. An 8 mM stock of *p*-CMB was prepared as described (Boyer, 1954) in 20 mM sodium phosphate, pH 6.9, and 400 mM $(NH_4)_2SO_4$. The concentration was determined spectrophotometrically using ϵ_{232} = 1.69 × 10^4 cm^{-1} M^{-1} in 50 mM sodium phosphate, pH 7.0 (Boyer, 1954). This stock was added to 50 ml of a suspension of membrane sheets (11 μM A103C) in 30 mM sodium phosphate, pH 6.9, and 0.025% NaN_3 at a 1.5-fold molar excess over protein. Incorporation of *p*-CMB was monitored during the reaction by determining the change in absorbance at 250 nm (Boyer, 1954) and was complete in 2 h. After ~15 h in the dark at room temperature, membranes were sedimented for 40 min at 24 000 rpm in a Beckmann 45Ti rotor (45000*g*) at 4 °C. The samples were washed twice by resuspending the pelleted membranes in 60 mL of 5 mM NaCl and centrifuging as above. The pellet was resuspended in ~100 μL of H_2O containing 0.025% NaN_3.

Spectroscopy. UV/visible absorption spectra were obtained as described (Krebs et al., 1993) from membranes suspended in 30 mM sodium phosphate, pH 6.9, at 20 °C. Dark adaptation under these conditions was monitored for 12 h, and the kinetics were fit with a single-exponential decay. The kinetics of the photocycle and of proton release were measured as described (Otto et al., 1990) in 150 mM KCl, pH 7.3, at 22 °C. The extent of *p*-CMB labeling was calculated from the molar ratio of A103C protein to mercaptide formed. The concentration of A103C-MB was calculated from the light-adapted spectrum assuming the same extinction coefficient as wild-type bR, ϵ_{568} = 6.27 × 10^4 cm^{-1} M^{-1} (Rehorek & Heyn, 1979). The concentration of mercaptide formed was determined from the difference at 236 nm between the light-adapted spectra of A103C-MB and A103C (normalized at 568 nm) by using ϵ_{236} = 2.45 × 10^4 cm^{-1} M^{-1}. This value for the extinction coefficient was calculated from the change in A_{236} resulting from addition of a substoichiometric amount of *p*-CMB to A103C membranes.

X-ray Diffraction. X-ray diffraction measurements were performed with a rotating anode X-ray generator (Elliott-Marconi GX21) at 1.542 Å as described (Heyn et al., 1989). The powder diffraction patterns were recorded in the radial direction by a one-dimensional position-sensitive detector (Braun OED-50-M). Hydrated oriented membrane samples were prepared by drying a concentrated drop of purple membrane suspension on a 5 μm thick mylar support at 86% relative humidity. The oriented membrane films were mounted with the planes of the membranes perpendicular to the X-ray beam in a chamber that was kept at 100% relative humidity. The samples were equilibrated for 24 h in the constant humidity sample holder before the measurements. X-ray data were collected for 19 h in 1-h runs. By comparing the data from individual 1-h runs, systematic errors and drift in the detection electronics could be controlled. The measurements were performed at room temperature in the dark-adapted state with membrane samples containing 1 mg of bR in distilled water. In order to minimize differences in treatment between the labeled (A103C-MB) and unlabeled (A103C) samples, all operations such as centrifugation, film preparation, and drying were performed in parallel.

Data Analysis. Background subtractions were performed using linear or Gaussian functions. The integrated intensities were calculated by fitting the intensity profiles to Gaussian line shapes and were corrected by a Lorentz factor of $(h^2 + hk + k^2)^{1/2}$. The sum of the intensities differed by only 3% between the labeled and unlabeled samples. The factor required to scale the two data sets was accordingly very close to one. Fourier difference maps were calculated from the intensity differences using the phases and the intensity ratios for reflections with the same value of $h^2 + hk + k^2$ from electron microscopy (Henderson et al., 1986). The justification for this procedure has been discussed in detail (Plöhn & Büldt,

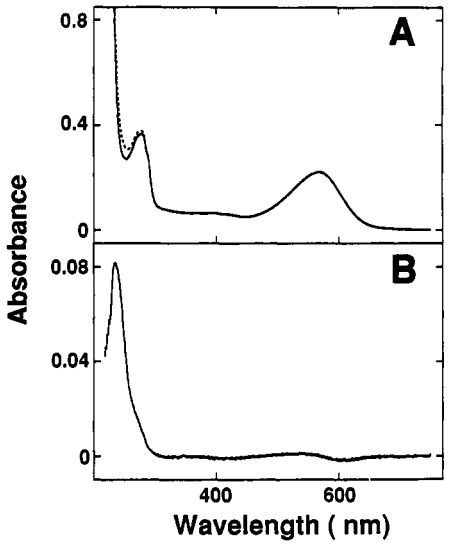

FIGURE 2: (A) Light-adapted spectra of A103C (—) and A103C-MB (- - -), normalized at 568 nm. Membrane preparations suspended in 30 mM sodium phosphate, pH 6.9, at 20 °C were illuminated (5 min, >530 nm light). (B) Difference spectrum obtained by subtracting the A103C spectrum from the A103C-MB spectrum in panel A.

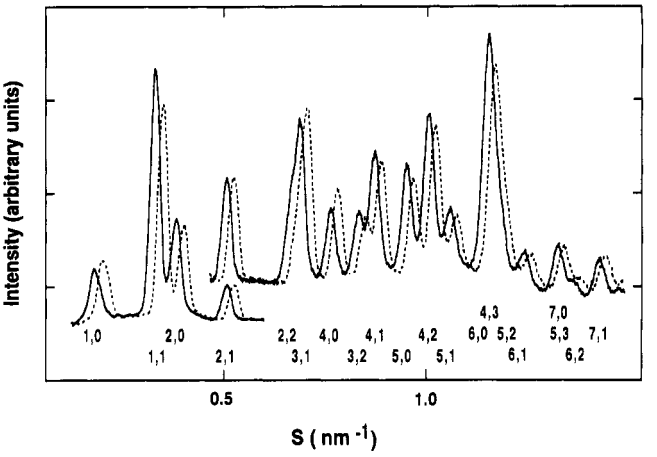

FIGURE 3: X-ray diffraction patterns of A103C (—) and A103C-MB (- - -) before Lorentz correction as a function of the scattering vector, $s = 2 \sin \theta/\lambda$. For clarity of presentation, the A103C-MB data set is slightly displaced to the right. The reflections from the hexagonal lattice are labeled by the indices (h,k). Beginning with the (2,1) reflection, the vertical scale has been expanded by a factor of 3.

1986). Experimentally, this approximation is supported by the excellent agreement of the structural information obtained by X-ray or neutron diffraction with that obtained by electron microscopy in those cases where a direct comparison is possible. These include determination of the in-plane position of the cyclohexane ring of the chromophore (Seiff et al., 1986a; Henderson et al., 1990) and measurement of the change in protein density in the bR to M transition (Koch et al., 1991; Subramaniam et al., 1993). The label position determined in this way from the Fourier difference map was used as the starting point for the refinement procedure (Dickerson et al., 1968; Seiff et al., 1986b).

RESULTS

Expression of a bR Cysteine Mutant in H. halobium. As a test case for heavy-atom labeling, we chose the bR mutant A103C (Greenhalgh et al., 1991), which contains a unique cysteine residue in the loop of five amino acids between transmembrane α-helices C and D (Figure 1). The short length of the C–D loop and the proximity of position 103 to an α-helix suggested this residue would be relatively immobile, an important requirement for localizing the heavy-atom label. In addition, nitroxide spin-labeling studies of A103C expressed in *Escherichia coli* indicated that position 103 is exposed to the aqueous environment and can be derivatized without affecting retinal binding or proton pumping (Greenhalgh et al., 1991). To obtain a preparation of A103C suitable for diffraction studies, the protein was expressed in a recombinant strain of *H. halobium* constructed by gene replacement (Krebs et al., 1993). The protein was purified to 98% homogeneity in a form similar to the purple membrane.

Heavy-Atom Labeling of A103C. Purified A103C in membranes was treated with *p*-CMB, a sulfhydryl-specific mercury reagent that can be used for spectroscopic determination of cysteine (Boyer, 1954). The labeled sample, A103C-MB, showed greater absorbance in the ultraviolet region compared to the unlabeled sample, A103C (Figure 2A). The corresponding difference spectrum (Figure 2B) was similar to the spectrum of cysteine mercuribenzoate (Boyer, 1954), consistent with incorporation of the label. The level of incorporation determined from difference spectra was 0.88 ± 0.06 mol mercuribenzoate per mol A103C. No incorporation was observed in wild-type bR under the same conditions, indicating that labeling was specific.

Functional Characterization of A103C and A103C-MB. The A103C and A103C-MB membrane samples had functional properties similar to the purple membrane. Wild-type bR in purple membrane has a visible absorption maximum of 568 nm in the light and shifts to 558 nm in the dark with a decrease in extinction (Stoeckenius et al., 1979). The visible spectra of light-adapted A103C and A103C-MB (Figure 2A) were nearly identical with each other and with that of wild-type bR. A very minor spectral shift was apparent in the visible region of the difference spectrum (Figure 2B). The dark-adapted spectra of these samples were also nearly identical (data not shown). The rate of dark adaptation of A103C, A103C-MB, and wild-type bR was comparable and could be fit by a single-exponential decay with a $t_{1/2}$ of 93, 88 and 93 min, respectively. The kinetics of the photocycle of A103C, A103C-MB, and wild-type bR were measured at a number of wavelengths and were very similar. For example, at 410 nm the mean rise and decay times of M were 99 μs/3.4 ms, 96 μs/3.7 ms, and 89 μs/3.7 ms for A103C, A103C-MB, and wild type, respectively. The proton release times for these samples, as measured with the pH-sensitive dye pyranene, were also quite close: 973, 862, and 947 μs, respectively.

X-Ray Diffraction of A103C and A103C-MB. The diffraction patterns of labeled and unlabeled A103C (Figure 3) were indexed on a hexagonal P_3 lattice with unit cell dimensions of 62.2 ± 0.2 and 62.2 ± 0.2 Å, respectively. The unit cell dimensions are the same within experimental error and equal to the value established for wild-type purple membrane of 62.4 (Glaeser et al., 1985). Figure 3 shows that X-ray diffraction peaks were observed out to the (7,1) reflection, which corresponds to a resolution of 7.2 Å. The data analysis was facilitated by the fact that the background scattering from the two samples was virtually identical (Figure 3). Positive and negative intensity differences due to the mercuribenzoate group can be easily recognized. This is most noticeable when comparing the relative intensities of neighboring reflections. For example, the intensity ratio of the (4,0) and (3,1) reflections is clearly larger in the labeled sample.

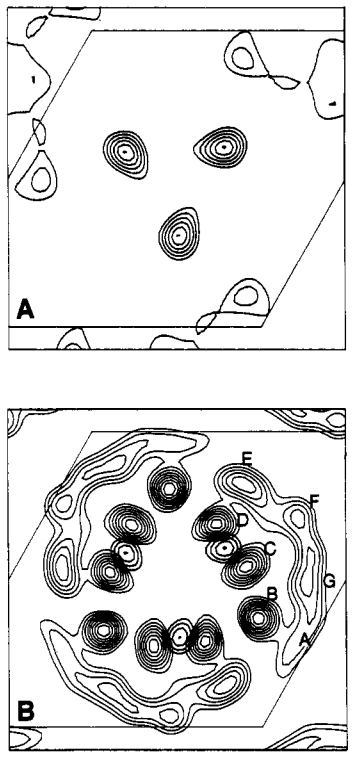

FIGURE 4: (A) Two-dimensional difference density map showing the in-plane position of the mercuribenzoate label bound at Cys-103. Negative contour lines were omitted. The six solid contour lines range from 50 to 99% of the positive difference density. (B) Superposition of the label position from panel A (the four highest contour lines representing 70, 80, 90, and 99% of the positive density; bold lines) on the projected structure of A103C determined from the X-ray intensities of Figure 3 (thin lines). The seven transmembrane α-helices are labeled A–G.

In two independent X-ray experiments, the main intensity changes were clearly above the noise level. The overall relative intensity change, $\Sigma|\Delta I|/\Sigma I$, between the A103C and A103C-MB samples before Lorentz correction was 8.3 and 7.9% for the two experiments, respectively. The degree of similarity between these two data sets was judged by computing the sample correlation coefficient as described (Glaeser et al., 1986). The correlation coefficient of 0.92 indicates a high degree of similarity between the two sets of intensity differences.

Refinement of the Mercury Label Position. Using the data of Figure 3, the electron density of the label was calculated as described under Materials and Methods. The resulting electron density map after refinement is shown in Figure 4A. The three difference maxima correspond to the three label positions. Fractional coordinates are defined with the origin in the center of the unit cell and with x and y increasing along the oblique and horizontal axes from top to bottom and from left to right, respectively. In terms of these coordinates, the refined label positions (x, y) are (0.200, 0.104) and (0.198, 0.106) for the two independent experiments. The small distance of only 0.24 Å between these two points is a measure of the good experimental reproducibility. The refined label position was independent of the position chosen for starting refinement within an 8 Å radius of the final position. To test whether the observed intensity changes and the corresponding label density have the magnitude expected for a single mercury atom per A103C monomer, model calculations were performed as described (Seiff et al., 1986b; Plöhn & Büldt, 1986). The ΔF values for the model calculation agree well with those from the refinement, indicating that the observed difference in electron density is due to the mercuribenzoate label. The highest contour lines of the label density are drawn superimposed on the density map of A103C in Figure 4B. The projected position of the mercury label attached to Cys-103 is between transmembrane α-helices C and D (Henderson et al., 1990).

DISCUSSION

By combining site-specific mutagenesis, heavy-atom labeling, and X-ray diffraction, we have determined the location of a single amino acid residue within the loop connecting transmembrane α-helices C and D of bR. A unique cysteine residue was introduced at position 103 of bR by site-specific mutagenesis. Two-dimensional crystals of the mutant protein were obtained from a recombinant *H. halobium* strain constructed by gene replacement (Krebs et al., 1993). The crystalline protein was labeled with a sulfhydryl-specific reagent containing mercury, which was then localized by X-ray diffraction using established methods. The use of site-specific mutagenesis to introduce cysteines for heavy-atom labeling was originally demonstrated with T4 lysozyme, a soluble protein for which three-dimensional crystals are available (Dao-Pin et al., 1987). In this work, we have shown that the same strategy can be used for structural studies of an integral membrane protein in two-dimensional crystals.

Our results indicate that the unique cysteine residue of A103C can be labeled efficiently in the two-dimensional lattice form of the protein. The *p*-CMB label was incorporated in A103C with a stoichiometry of 0.9 mol of mercuribenzoate per mol of bR, consistent with reaction of a single sulfhydryl group with the mercury compound. The absence of a *p*-CMB reaction with wild-type bR and the presence of a single mercury peak per A103C monomer in the diffraction analysis indicated this reaction was specific for cysteine. This result was expected, since mercury compounds form complexes preferentially with protein sulfhydryl and imidazole groups (Petsko, 1985), and bR has no histidine residues. The high efficiency of A103C labeling was remarkable. Studies of water-soluble proteins have indicated that highly exposed cysteines react poorly with mercury compounds (Dao-Pin et al., 1987; Tucker et al., 1989). These studies concluded that partially exposed residues in a surface crevice are most suitable for derivatization. Thus, the efficient labeling of A103C suggests position 103 is not fully exposed to the aqueous environment. This supports nitroxide spin-label experiments, which show that position 103 is exposed, but not completely mobile (Greenhalgh et al., 1991).

Before interpreting the X-ray diffraction results, we established that labeled and unlabeled A103C were isomorphous with wild-type bR. Several sensitive assays indicated that the functional properties of A103C and A103C-MB were identical to those of wild-type bR within experimental error: (i) the light- and dark-adapted visible spectra were essentially the same, (ii) the rates of dark adaptation were identical, (iii) the rise and decay times of the M intermediates were the same, and (iv) the proton release times were nearly indistinguishable. The samples were also structurally similar. Both A103C and A103C-MB formed a hexagonal lattice of unit cell dimension 62.2 Å like that of wild-type bR in the purple membrane. On the basis of these criteria, neither the cysteine substitution at position 103 nor the subsequent derivatization with mercuribenzoate seems to perturb the system. These results are not unexpected, considering that the labeling conditions were very mild and that the cysteine substitution was made in an exposed loop where bulky groups could be accommodated.

The X-ray diffraction patterns of A103C and A103C-MB exhibit distinct intensity differences due to the presence of the mercuribenzoate group (Figure 3), allowing the straightforward determination of the label position (Figure 4). Model calculations have shown that with the moderate resolution of our data and the assumptions of the data analysis the label position can be determined with an accuracy of ±1 Å (Plöhn & Büldt, 1986). The difference in electron density corresponds in strength to that expected for a single mercury atom. Figure 4B shows that the in-plane position of the labeled cysteine at position 103 is between helices C and D, exactly as expected for an amino acid in the C–D loop. Apparently, at least the part of the short C–D loop that includes 103 is sufficiently structured to yield a clear-cut difference density. A highly mobile loop would smear out the label density making it difficult to observe a defined position. One advantage of introducing a mercury label at a cysteine residue is that the mercury atom is only three bonds away from the main chain C_α atom. Thus, the C_α atom of the cysteine at position 103 must fall within 4.5 Å of the peak maximum in the Fourier difference map.

The strategy of obtaining structural information by derivatizing a unique cysteine with a heavy atom may be continued with other residues of the C–D loop and with the other loops provided they are immobile. Of considerably greater interest and promise, however, is the possibility of using these labels at well-defined positions to monitor structural changes that occur during the bR photocycle. Changes in the protein density have been observed in the light-induced transition from the ground state to the M intermediate near helices B, F, and G (Koch et al., 1991; Subramaniam et al., 1993). These functionally important structural changes may be better characterized by specific labeling at strategic sites.

The approach described here is also attractive for refining the structure of other integral membrane proteins for which three-dimensional crystals are not available. The method can significantly advance the interpretation of an electron density map, since the heavy-atom location can be determined with an accuracy greater than the resolution of the diffraction measurements. Although the C_α atom of the labeled cysteine can be localized only to within 4.5 Å of the heavy atom, this would be sufficient to correlate regions of density in the structural map with the amino acid sequence. Analysis of a few well-chosen cysteine mutants could provide positional constraints for assigning and orienting transmembrane segments and loops. The approach requires (i) phase information from electron imaging and (ii) milligram amounts of mutant proteins modified to contain a unique, derivatizable cysteine residue. These criteria have already been met for a number of prokaryotic integral membrane proteins (Kühlbrandt, 1992) and may be achieved with eukaryotic proteins as expression systems are improved.

ACKNOWLEDGMENT

We thank Judy Carlin for her excellent assistance in preparation of the manuscript and Duncan Greenhalgh for useful discussions. We thank Robert Griffin for critical reading of the manuscript. We also thank Ulrike Alexiev and Harald Otto for performing the flash photolysis measurements.

REFERENCES

Amos, L. A., Henderson, R., & Unwin, P. T. N. (1982) *Prog. Biophys. Mol. Biol. 39*, 183–231.
Boyer, P. D. (1954) *J. Am. Chem. Soc. 76*, 4331–4337.
Dao-Pin, S., Alber, T., Bell, J. A., Weaver, L. H., & Matthews, B. W. (1987) *Protein Eng. 1*, 115–123.
Dickerson, R. E., Weinzierl, J. E., & Palmer, R. A. (1968) *Acta Crystallogr. B24*, 997–1003.
Engelman, D. M., Henderson, R., McLachlan, A. D., & Wallace, B. A. (1980) *Proc. Natl. Acad. Sci. U.S.A. 77*, 2023–2027.
Glaeser, R. M., Jubb, J. S., & Henderson, R. (1985) *Biophys. J. 48*, 775–780.
Glaeser, R. M., Baldwin, J., Ceska, T. A., & Henderson, R. (1986) *Biophys. J. 50*, 913–920.
Greenhalgh, D. A., Altenbach, C., Hubbell, W. L., & Khorana, H. G. (1991) *Proc. Natl. Acad. Sci. U.S.A. 88*, 8626–8630.
Henderson, R., Baldwin, J. M., Downing, K. H., Lepault, J., & Zemlin, F. (1986) *Ultramicroscopy 19*, 147–178.
Henderson, R., Baldwin, J. M., Ceska, T., Zemlin, F., Beckmann, E., & Downing, K. H. (1990) *J. Mol. Biol. 213*, 899–929.
Heyn, M. P., Dudda, C., Otto, H., Seiff, F., & Wallat, I. (1989) *Biochemistry 28*, 9166–9172.
Klein, C., Vogel, W., Bender, H., & Schulz, G. E. (1990) *Protein Eng. 4*, 65–67.
Koch, M. H. J., Dencher, N. A., Oesterhelt, D., Plöhn, H.-J., Rapp, G., & Büldt, G. (1991) *EMBO J. 10*, 521–526.
Krebs, M. P., Hauss, T., Heyn, M. P., RajBhandary, U. L., & Khorana, H. G. (1991) *Proc. Natl. Acad. Sci. U.S.A. 88*, 859–863.
Krebs, M. P., Mollaaghababa, R., & Khorana, H. G. (1993) *Proc. Natl. Acad. Sci. U.S.A. 90*, 1987–1991.
Kühlbrandt, W. (1992) *Q. Rev. Biophys. 25*, 1–49.
Mathies, R. A., Lin, S. W., Ames, J. B., & Pollard, W. T. (1991) *Annu. Rev. Biophys. Biophys. Chem. 20*, 491–518.
Nassal, M., Mogi, T., Karnik, S. S., & Khorana, H. G. (1987) *J. Biol. Chem. 262*, 9264–9270.
Otto, H., Marti, T., Holz, M., Mogi, T., Stern, L. J., Engel, F., Khorana, H. G., & Heyn, M. P. (1990) *Proc. Natl. Acad. Sci. U.S.A. 87*, 1018–1022.
Petsko, G. A. (1985) *Methods Enzymol. 114*, 147–156.
Plöhn, H.-J., & Büldt, G. (1986) *J. Appl. Crystallogr. 19*, 255–261.
Rehorek, M., & Heyn, M. P. (1979) *Biochemistry 18*, 4977–4983.
Schertler, G. F. X., Villa, C., & Henderson, R. (1993) *Nature 362*, 770–772.
Seiff, F., Westerhausen, J., Wallat, I., & Heyn, M. P. (1986a) *Proc. Natl. Acad. Sci. U.S.A. 83*, 7746–7750.
Seiff, F., Wallat, I., Westerhausen, J., & Heyn, M. P. (1986b) *Biophys. J. 50*, 629–635.
Stock, A. M., Mottonen, J. M., Stock, J. B., & Schutt, C. E. (1989) *Nature 337*, 745–749.
Stoeckenius, W., & Bogomolni, R. A. (1982) *Annu. Rev. Biochem. 52*, 587–616.
Stoeckenius, W., Lozier, R. H., & Bogomolni, R. A. (1979) *Biochim. Biophys. Acta 505*, 215–278.
Subramaniam, S., Gerstein, M., Oesterhelt, D., & Henderson, R. (1993) *EMBO J. 12*, 1–8.
Toyoshima, C., Sasabe, H., & Stokes, D. L. (1993) *Nature 362*, 469–471.
Tucker, A. D., Baty, D., Parker, M. W., Pattus, F., Lazdunski, C., & Tsernoglou, D. (1989) *Protein Eng. 2*, 399–405.
Unwin, N. (1993) *J. Mol. Biol. 229*, 1101–1124.